Surface Analysis and Structures Spherical Crystals of Very Clean Au, Cu and Au-Cu Alloys Grown from a Drop of Melt

B. Grosser and E. Menzel

Institut für Halbleiterphysik und Optik, Technische Universität Braunschweig

Z. Naturforsch. **40 a,** 479 – 484 (1985); received February 23, 1985

Surface impurities on spherical Au and Cu crystals grown from a drop of melt on graphite in UHV were analyzed by Auger electron spectroscopy after the metals had been cleaned by melting resp. roasting in air. Crystals of Au-Cu alloys grown by the same technique show enrichment of the less abundant component.

The well known reconstructions Au(001)(5×20) and Au(111)(23×1) could not be detected by RHEED and LEED on cleaned Au crystals. But both structures were confirmed on crystals of Au + 45 at ppm Cu. Au(110)(1×2) was present on cleaned and weakly Cu alloyed Au crystals.

1. Introduction

Experimental results in surface physics depend on surface preparation. Techniques different from the common one – sputtering and annealing – may give new information. Since 1953 we have used surfaces of spherical metal crystals (diameters 2 – 4 mm) grown by solidification of a drop of melt in a temperature gradient without any further surface preparation. Their spherical shape provides an overview of the surfaces of all crystallographical orientations [1]. Crystals of copper, silver and gold grown on spectral graphite have high crystal quality as shown by electron diffraction. The low indexed flats (111) and (001) and the other curved areas are smooth at least in light-optical sense [1]. Alloying Au with 100 at ppm Cu destroys this smoothness [7]. In order to check the cleanliness by an other method we have started Auger electron spectroscopy (AES) with a four grid retarding field analyser (Vacuum Generators), with primary electrons up to 4 keV and suitable modulations between 2 and 6 V. In the present work former investigations on purified gold [2] are extended to copper and to Au-Cu alloys. Electron diffraction in this system is reported additionally.

Our crystals do not adhere to the graphite support. Therefore the usual arrangement for AES and electron diffraction had to be modified. Now the AES/LEED gun with the grid system is above the crystal and the RHEED axis is horizontal. The metal vapour of the melting specimen could damage the AES system. Therefore a protecting cage is pushed over the specimen when it is on higher temperatures. A mirror beneath the specimen gives a look on the LEED screen.

2. AES on Gold and Copper

High purity gold was chemically etched, then melted and solidified. AES showed, apart from the gold signals, a strong carbon peak (272 eV) and a small silicon peak (92 eV). The crystals had a comparatively rough surface [2]. Purification was possible by melting the gold in air. In a temperature gradient spherical gold crystals grow in air with quite smooth surfaces. AES was performed without any further melting or after remelting and solidification on spectral graphite in 10^{-7} Pa. In both cases the carbon peak was lowered by a factor 1/5, the silicon peak had dissappeared, and in spite of melting in air no nitrogen or oxygen peaks or other ones were detected [2]. A peak at 150 eV does not belong to sulphur but to gold because its intensity fits to the other Au peaks. Our results on our Au crystals were confirmed after transportation in air by AES with a cylindrical mirror analyser in the Physikalisches Institut, Universität Hohenheim [2]; especially no oxygen was detected at 510 eV.

Earlier work has dealt with spherical copper crystals (see [3]) grown on graphite in technical or UH vacuum by the same technique. Before melting, etching in HNO_3 followed by HCl was necessary. Recently the cleanliness of Cu could be improved

---

Reprint requests to Prof. E. Menzel, Institut für Halbleiterphysik und Optik, Techn. Universität, Postfach 33 29, D-3300 Braunschweig, Germany.

0340-4811 / 85 / 0500-0479 $ 01.30/0. – Please order a reprint rather than making your own copy.

Table 1. Average surface impurities in at% on several Au and Cu crystals grown in UHV without or after precleaning by oxygen, or grown in air only. Numbers of samples in brackets.

	Au			Cu	
	melting in UHV only (3)	melting in air, then melting in UHV (7)	melting in air only (11)	melting in UHV only (5)	roasting in air, then melting in UHV (4)
C	22 ± 5	5 ± 1	5 ± 1	17.5 ± 2	9.7 ± 0.7
S	–	–	–	3.7 ± 0.3	2.1 ± 0.3
Si	1	–	–	–	–

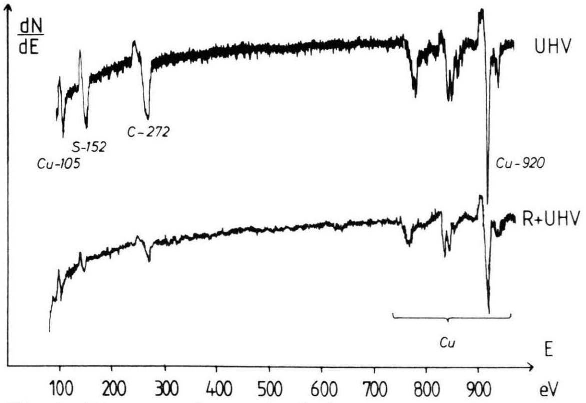

Fig. 1. AE spectra from spherical copper crystals grown on graphite in UHV from a drop of melt. UVH: without roasting in air; R + UHV: after roasting the Cu piece in air.

further by roasting the etched pieces in air without melting them. The Cu oxides are reduced by the following melting in vacuum on graphite [3]. Figure 1 shows AE spectra from Cu crystals grown by solidification of a drop of melt in UHV without and after precleaning in air. By roasting the carbon sulphur peaks are lowered by a factor 1/2. By taking in account the AES sensitivities [4], the surface concentrations of the impurities have been calculated from the peak-to-peak heights *I* (Table 1).

In past times particles of slag moving on the drops of melt gave problems, but on the other hand they could be used for probing the depth of melt layers on Cu just below the melting point [5]. These slags were diminished by the chemical etching and the air treatment. But we could not surely identify the slags by AES.

3. AES on Au-Cu Alloys

Spherical crystals of different Au-Cu alloys were grown from a drop of melt as described in [6, 7]. By observing the contrast of the thermal luminosity just below the point of solidification the liquid-solid interface can be seen.

On crystals with more than 100 at ppm Au or Cu, surface dendrites were indicated by unevenness of the interface, and at room temperature by a characteristic unevenness of the surfaces [7]. Crystals with more than 2 at% Au or Cu show growing darker islands during solidification; this and the surface topography of the cold specimens are characteristic for volume dendrites reaching the crystal surfaces [7]. Dendritic growth in an alloy causes decomposition lateral to the dendrites.

By observation of the liquid-solid interface on weak alloys up to 2000 at ppm Au or Cu it was found that most of the crystal surfaces are covered by a layer of melt 40 nm to a few μm deep. In this layer the diluted component (Au or Cu) is enriched [8]. Only "black areas" around the (111) and (001) poles of the crystal spheres remain nearly free from this surface melt. These areas show a tendency for lateral cleaning [8]. The surface enrichment observed on weak alloys will be present also on higher alloyed crystals.

The deep surface enrichment connected with solidification must not be confused with the surface segregation at a monolayer level as it was observed and calculated for binary alloys equilibrized at several hundred degrees under the melting point [9, 10]. This surface segregation decreases corresponding to equilibrium with raising temperature [11].

But on the other hand equilibrium on solids needs diffusion with sufficient temperature and

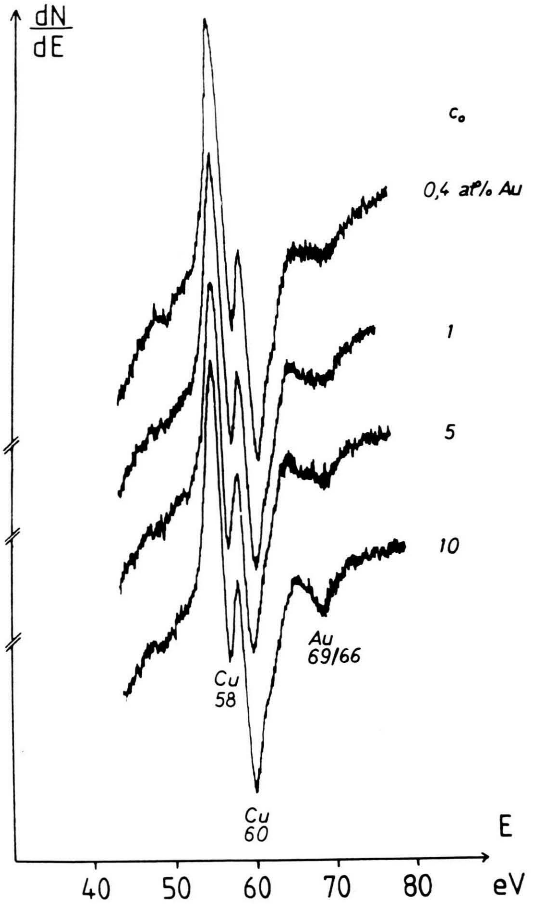

Fig. 2a. AE spectra from Au-Cu crystals with small weight-in concentrations c_0 of Au.

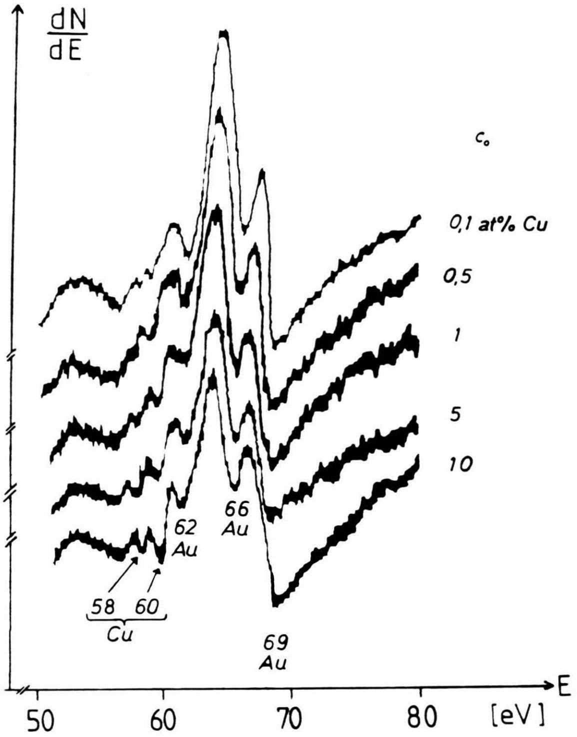

Fig. 2b. AE spectra from Au-Cu crystals with small weight-in concentrations c_0 of Cu.

time. Therefore we must expect a complex situation when we observe AES on our crystals at room temperature after solidification and cooling down within 30 min. The enriched deep surface melt and the inhomogeneous composition of the dendritic structure just below the melting point must be modified during cooling by the tendency of the solid surface to follow the equilibria of surface segregation at medium temperatures.

AE spectra were taken from alloys on both sides of the Au-Cu system. For reference the specimens could change place with an Au foil which was prepared by rolling pure Au crystals between sheets of steel or molybdenum and by roasting in air for final cleaning. The AE spectra of the Au foils agreed with the spectrum of purified crystals. The peak Au-69/66 gave the reference.

Figure 2 shows AE spectra from different Au-Cu alloys. Beside the known peaks from carbon and sulphur in Cu rich alloys and from carbon in Au rich alloys no other impurities were indicated.

Figure 3 depicts the peak-to-peak heights I of Au-69/66 and Cu-60 as functions of the weight-in concentrations c_0. The I values for Au in Cu-rich alloys were averages from four different spectra and for Cu in Au-rich ones from five spectra. Using the known sensitivities [4] of the AES signals, surface concentrations c_s of the diluted components were calculated. From these follow the ratios of segregation $a = c_s/c_0$ on our specimens at room temperature. In Table 2 these results are compared with a-values found in [8] closely below the melting point and with a-values calculated for surface segregation in the first monolayer at 850 °C [9].

Table 2. Ratios of surface segregation *a* for the diluted components on Au-Cu alloys.

		Weight-in concentrations in at%							
		0.01	0.1	0.2	0.4	0.5	1	5	10
Y. W. Lee and H. J. Aaronson (1980) [9]	Au Cu					← tendency for increasing *a*			4.7 5.7
M. Schneegans (1983) [8]	Au Cu	7.8 6.6		3.7 3.3					
This paper	Au				10 ± 3		6.3 ± 1.0	1.6 ± 0.1	1.0 ± 0.1
	Cu		< 20 ± 4			6.6 ± 1.4	4.5 ± 1.0	1.4 ± 0.1	1.0 ± 0.1

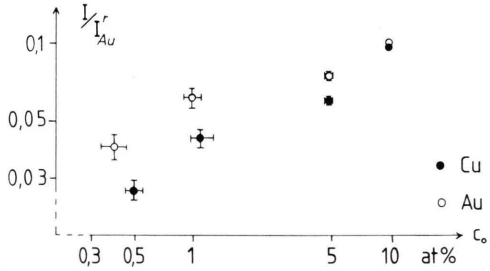

Fig. 3. Mean peak-to-peak heights *I* of the diluted component with respect to the Au foil.

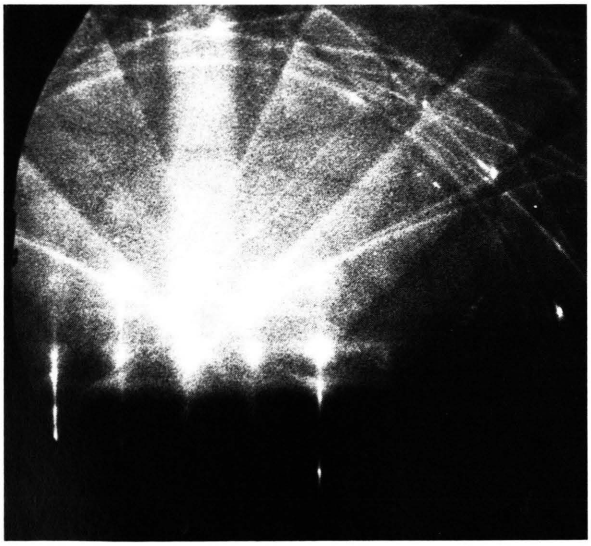

Fig. 4. RHEED diagram (30 keV primary beam in [001]) from Cu(001) after cleaning the Cu by roasting in air and melting it on graphite in UHV. The doubling of Kikuchi lines (002) and (004) described in [14] is depicted again.

As discussed, these three sorts of segregation have different physical origin; they were evaluated in different regions of c_0. But they show all enrichments of the diluted component Au or Cu growing with decreasing weight-in concentrations.

The low energy AES peaks Au-69/66 and Cu-60 have a low escape depth and give concentrations only from the first monolayer, about 0.5 nm deep. We could additionally use the peak Cu-920 having an escape depth of about 1.3 nm. For $c_0 = 10$ at% Cu both peaks gave the same enrichment but for 4.9 at% Cu *a* amounted to 1.4 for a depth of 0.5 nm and 1.2 for 1.3 nm. This tendency for higher enrichments in the first layer fits the theory of segregation on solid surfaces [9]; the enrichments become more pronounced at lower weight-in concentrations.

The electron probe of our AES apparatus has a diameter of 0.5 mm; therefore no lateral resolution of inhomogenous surface concentrations as based on dendrites was possible. All spectra were taken on and near the "north-pole" of our crystal spheres without showing systematic changes.

4. Electron Diffraction: Surface Reconstructions

The measurements by AES should supplement foregoing observations and results in respect to surface segregation using optical observations. But our specimens and apparatus permitted additional experiments using electron diffraction. What follows is a sketch of some experimental results, they may be controversial to some current opinions.

Many investigations of copper crystals by electron diffraction have shown their unreconstructed ("naive") surfaces corresponding to the bulk lattice.

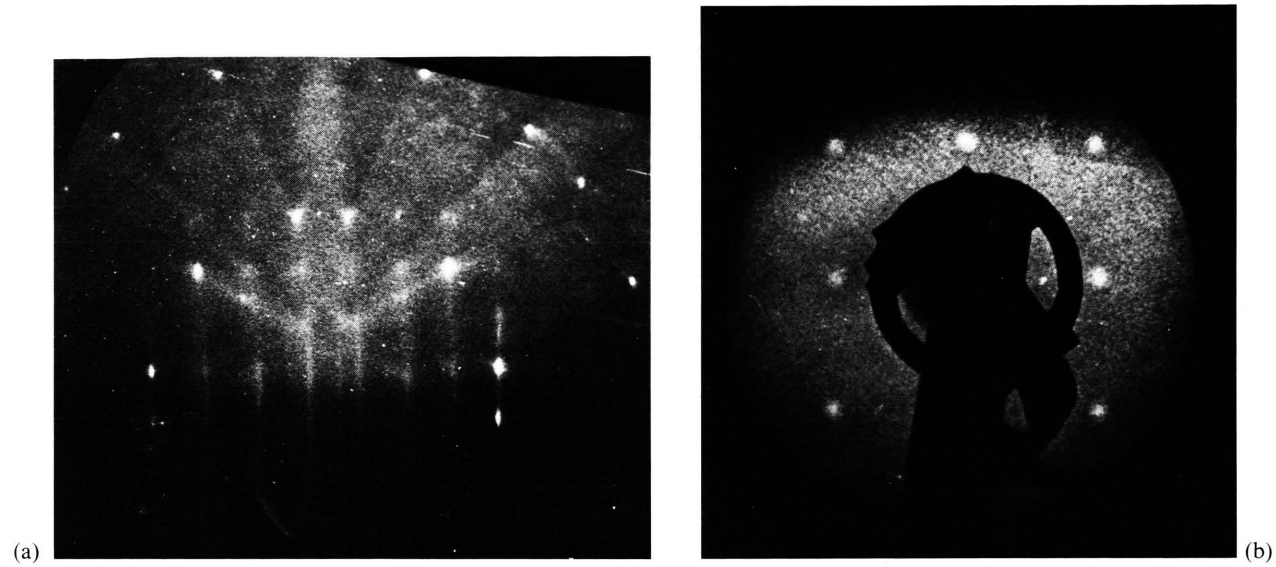

Fig. 5. (a) RHEED (30 keV primary beam in [001]) and (b) LEED (94 eV) diagrams from Au(001) after premelting the gold in air and remelting it on graphite in UHV.

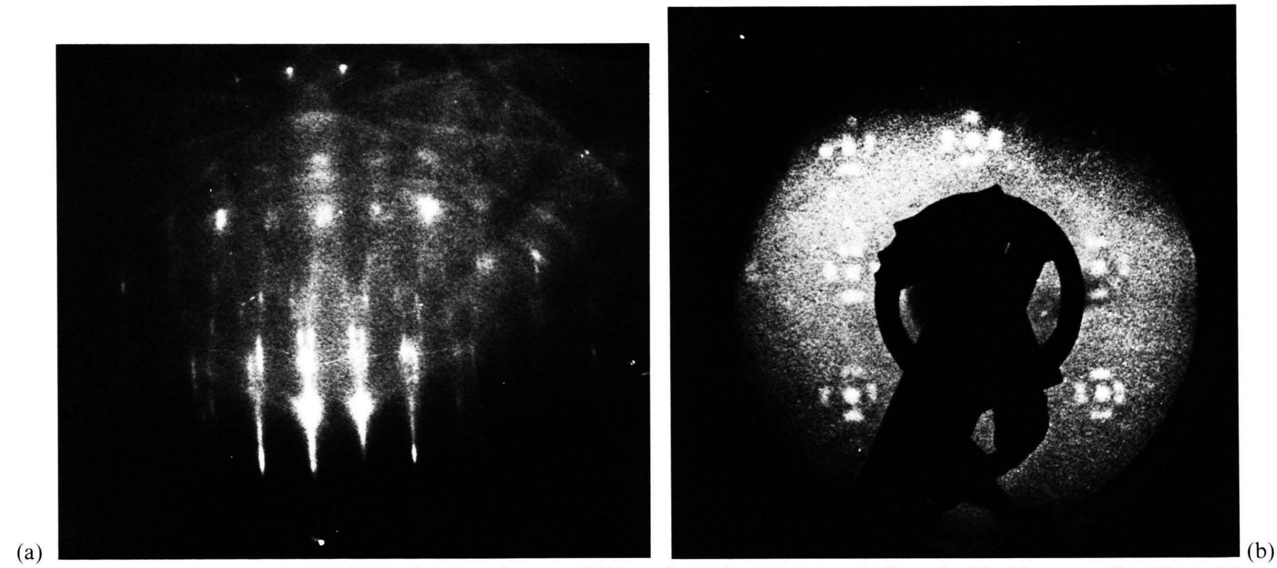

Fig. 6. (a) RHEED and (b) LEED diagrams from a (001) surface of a gold crystal alloyed with 45 at ppm Cu. The gold was cleaned before as in Figure 5.

We observed them also on our spherical Cu crystals solidified from a drop of melt by RHEED (see [1, 12]) and by LEED [13]. Cleaning of the copper as described in Chapt. 2 did not produce any change (Fig. 4), which is not surprising. Direct recording of RHEED diagrams inside of an apparatus with technical vacuum represents more details [12, 14] than recording from the fluorescent screen of an UHV apparatus, but here contaminations are better avoided.

Contrary to the naive surfaces of copper and silver, reconstructions on Au surfaces were observed by several authors (see [15]). Also on our spherical crystals of gold the well known structure (001)(5×20) was observed before we used the cleaning of Au by premelting it in air [15]. These crystals have shown also the known structure (110)(1×2) and the new ones (111)(23×1), (227)(1×1), (551)(1×1) and reconstructions on (001) vicinal planes [15]. Later on the new structure (111)(23×1) was confirmed by several authors on differently prepared specimens with different methods, as reported recently [16].

Surprisingly the oxygen-cleaned Au crystals show only the naive structures (001)(1×1) of Fig. 5 and (111)(1×1) [17]. These results were confirmed on 5 crystals after melting in air only and on 8 crystals after premelting in air and remelting in UHV. Only the reconstruction (110)(1×2) appeared again on purified crystals [17]. We did not look for structures on (227) and (551).

Kikuchi patterns from Au observed by RHEED are much weaker than those from Cu because these patterns are related to the three-dimensional lattice; therefore some penetration of the electrons is necessary to produce Kikuchi patterns; this depth is much lower in Au than Cu due to the higher atomic number of Au.

In the past, Au(001)(5×20) was occasionally supposed to be introduced by impurities (see [15]), but that could never made be sure. As reported 1978 [18] the structure (5×20) was changed to (1×1) by a bombardment with oxygen or other ions. But after annealing (1×1) at 100 °C, (5×20) reappeared again. We do not think that the Au(001)(1×1) structure on our air melted crystals could be produced by a similar influence of oxygen, because we could not find any oxygen by AES. On the other hand, melting of our cleaned Au on graphite in UHV must remove traces of oxygen from the premelting more efficiently than annealing at 100 °C. The same argument must be considered looking on the results of Yagi et al. [19]. These authors observed the Au(111) superstructure in the electron microscope, there the characteristic fringe contrast became weak after the sample was exposed to air.

Now using our technique to prepare crystals of extremely diluted alloys [7] we looked for reconstructed surfaces on Au + 45 at ppm Cu. Figure 6 depicts RHEED and LEED diagrams from (001). They show the well known patterns of the Au(001) (5×20) reconstruction (with LEED e.g. [18]). In the same way also (111)(23×1) and the (110)(1×2) structures were observed again on weakly alloyed Au crystals [17]. This was also confirmed in a sequence of three cycles of melting and crystallisation of the specimen. The surface segregation [8] would produce a higher Cu concentration; but taking in account the self-cleaning of the Au(111) and (001) flats [8], the Cu concentration necessary for the surface reconstructions may be lower than the weight-in concentration of 45 at ppm Cu. AES from this extremely weak alloy was without any Cu signal. On the other hand we did not get satisfying results with electron diffraction from higher alloyed Au-Cu crystals because their homogeneity in respect of composition and surface topography was destroyed by the dendrites.

This work was supported by the Deutsche Forschungsgemeinschaft.

[1] E. Menzel, Rpt. Progr. Phys. **26,** 47 (1963).
[2] K. D. Stock and B. Grosser, J. Crystal Growth **50,** 485 (1980).
[3] M. Schneegans, E. Menzel, and M. Beier, Z. Metallkunde **73,** 692 (1982).
[4] L. E. Davis, N. C. McDonald, P. W. Palmberg, G. E. Rich, and R. E. Weber, Handbook of Auger Electron Spectroscopy, 2nd ed. Phys. El. Industries Inc., Eden Prarie, Minnesota 1976.
[5] K. D. Stock and E. Menzel, J. Crystal Growth **43,** 135 (1978); K. D. Stock, Surf. Sci. **91,** 655 (1980).
[6] K. D. Stock, M. Schneegans, and E. Menzel, Z. Metallkunde **71,** 293 (1980).
[7] M. Schneegans and E. Menzel, J. Crystal Growth **63,** 309 (1983).
[8] M. Schneegans and E. Menzel, J. Crystal Growth **63,** 315 (1983).
[9] Y. W. Lee and H. J. Aaronson, Surf. Sci. **95,** 227 (1980).
[10] M. J. Sparnaay and G. E. Thomas, Surf. Sci. **135,** 184 (1983).
[11] W. Losch and J. Kirschner, J. Vac. Sci. Technol. **15,** 1541 (1978).
[12] Chr. Menzel-Kopp and E. Menzel, Z. Naturforsch. **8a,** 499 (1953); Chr. Menzel-Kopp, J. Phys. Soc. Japan **17,** Suppl. B-II 76 (1961); L. Trepte, Chr. Menzel-Kopp, and E. Menzel, Surf. Sci. **8,** 223 (1967); L. Trepte, Z. Naturforsch. **23a,** 1241 (1968).
[13] E. Menzel and O. Schott, Surf. Sci. **8,** 217 (1967); O. Schott, Z. angew. Phys. **22,** 63 (1967).
[14] Chr. Menzel-Kopp and E. Menzel, J. Phys. Soc. Japan **17,** Suppl. B-II, 80 (1961).
[15] H. Melle and E. Menzel, Z. Naturforsch. **33a,** 282 (1978).
[16] G. Nihoul, K. Abdelmoula, and J. J. Métois, Ultramicroscopy **12,** 353 (1984).
[17] B. Grosser, Dissertation Techn. Universität Braunschweig 1984.
[18] J. F. Wendelken and D. M. Zehner, Surf. Sci. **71,** 178 (1978).
[19] K. Yagi, K. Takayanagi, K. Kobayashi, N. Osakabe, Y. Tanishiro, and G. Honjo, Surf. Sci. **86,** 174 (1979).